Holographic Lithography

DOI: 10.1002/anie.200901166

Holographic Fabrication of Microstructures with Internal Nanopatterns Using Microprism Arrays**

*Seung-Kon Lee, Hyo Sung Park, Gi-Ra Yi, Jun Hyuk Moon, and Seung-Man Yang**

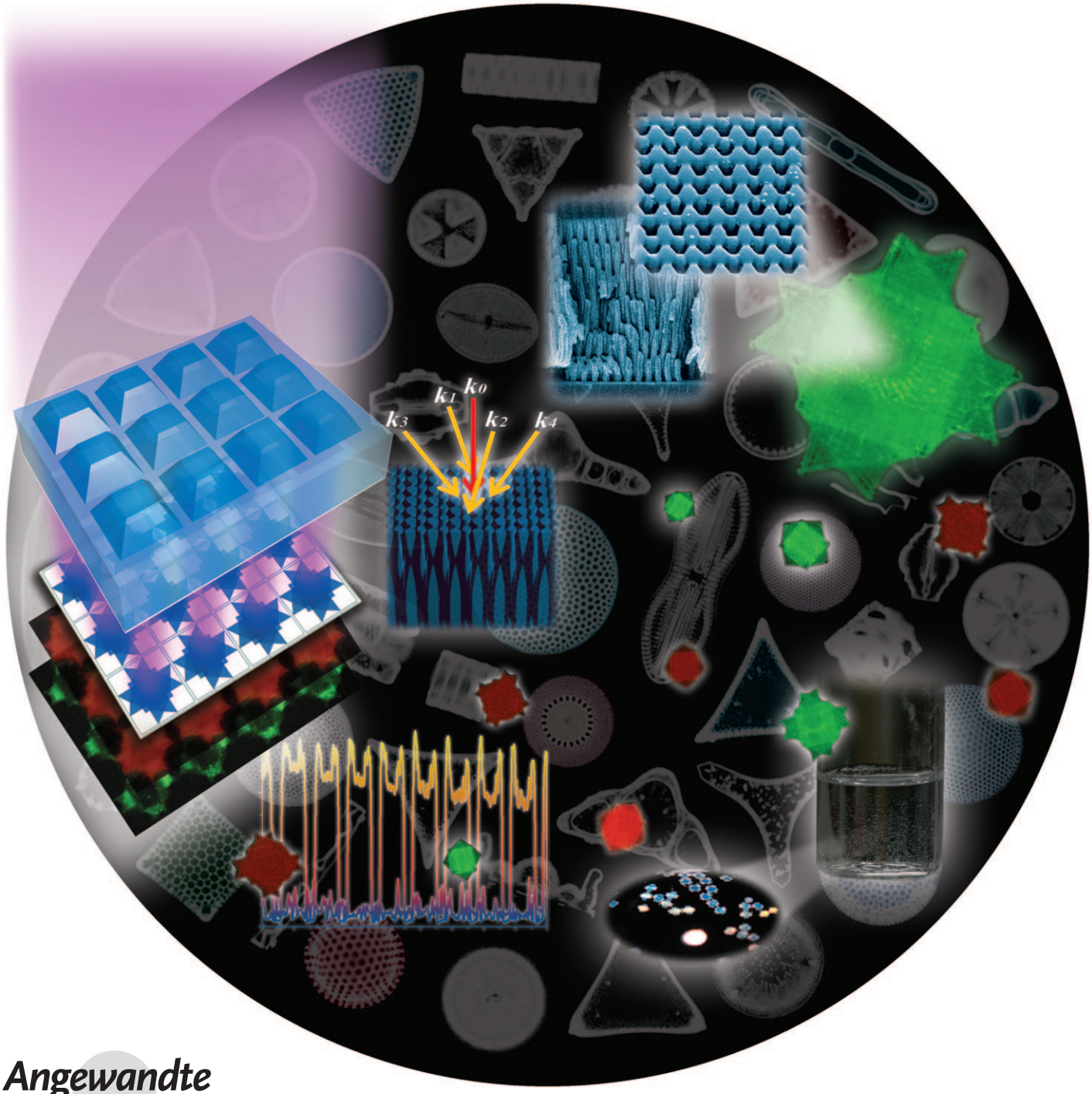

Recently, various synthetic materials with superlative properties have been developed by mimicking intricate nanoscopic structures in nature.[1] Bio-inspired multiscale nanostructures have attracted much attention owing to their potential applications in a wide range of areas from materials chemistry and life sciences to nanophotonics and electronics.[2–8] Despite recent advances in nanofabrication, the realization of such structures in a simple and controlled manner remains a challenge. Herein we report a facile method to construct well-controllable arrays of microstructures with internal nanopatterns in a single exposure using hierarchical interference of multiple laser beams through microprism arrays (MPAs). We also demonstrate mass production of free-floating microparticles with nanoscale patterns by releasing the MPA-derived microstructure arrays from the substrate. These microparticles resemble diatomaceous algae both in their structural features and in their highly efficient fluorescence, which suggests various applications including in situ diagnosis, bio-imaging, and biochemical detection and identification.[9–13]

Materials with periodic nanostructures have a variety of uses owing to their physical and chemical properties as well as their unique morphologies.[7,8,14,15] A number of methods has been developed for fabricating periodic nanostructures, including colloidal self-assembly, nanoimprinting, direct laser writing, electron-beam lithography, phasemask lithography (PML), and holography lithography (HL).[8,16–20] Among them, PML and HL have the advantage of being simple and rapid methods using laser interference patterns as masks to fabricate three-dimensional (3D) defect-free nanostructures.[19–20] In particular, Rogers and his colleagues have developed a variety of 3D nanostructures using a single-step exposure through a conformable phase mask and demonstrated a few promising applications, such as the fabrication of quasi-crystalline materials, graded photonic crystals, and organic-light emitting devices.[21–24] Although these conventional interference lithography methods have successfully produced 3D bulk structures with nanoscopic internal features or free-standing simple microparticles, it remains a challenge to construct patterned arrays of microstructures or free-standing microparticles with nanoscopic internal features in simple and controllable ways.[25–28] Herein, we report a new strategy for fabricating periodic arrays of microstructures with internal nanopatterns or free-standing microparticles with nanoscopic internal structures using hierarchical interference patterns of microprism arrays (MPAs) instead of a single macroscale prism.[29] In the MPA-based HL, a single laser beam is split into an array of multibeams by an MPA with microscale features. The beams refracted by a single microprism create interference patterns with nanoscopic features, as shown schematically in Figure 1. Therefore, our MPA-based HL has a few advanced features of practical significance over the conventional HL techniques. First, our MPA-based HL can construct controllable arrays of microstructures with nanoscopic internal patterns in a single exposure without employing a complicated setup of laser beams and optical components. Second, our strategy enables mass production of highly efficient, free-standing fluorescent microparticles with internal periodic nanostructures by releasing the arrayed microstructure patterns from the substrate. These microparticles resemble diatomaceous algae and exhibit highly sensitive fluorescence emissions, which are essential for probing for pH value, metal pollutants, and gases.[9–13]

Microprisms were made of transparent polydimethylsiloxane (PDMS) and arrayed on a 150 μm thick microscope cover glass. The patterned array of microprisms with square-pyramidal frustum shape was replicated by soft lithography from the primary silicon master, which was fabricated using an anisotropic etching process. A laser beam passed through each microprism was divided into five beams owing to the refraction at each face of the microprism (Figure 1). A laser beam introduced normal to the platform face resulted in perpendicular waves with $\boldsymbol{k}_0$ vector. Slanted side-beams with wave vectors $\boldsymbol{k}_1$–$\boldsymbol{k}_4$ resulted from refraction at the side faces of the microprism. Figure 1b illustrates the superimposition of multiple beams through a truncated pyramidal MPA. The overlapped silhouette image from a single microprism could be divided into several subsections according to the number of the superimposed beams $\boldsymbol{k}_0$–$\boldsymbol{k}_4$, which depends on the distance from the bottom of the MPA. We found that the area of five-beam interference was largest at around 150 μm from the bottom of the MPA. In Figure 1c, 3D five-beam interference nanostructure was illustrated by solving the interference equation with the corresponding wave vectors $\boldsymbol{k}_0$–$\boldsymbol{k}_4$. In this case, lower-dimensional interference structures appeared at the extended edges.

The 3D interference patterns from the MPA can be transferred to the photoresist material. Figure 2 shows scanning electron microscope (SEM) and optical microscope (OM) images of the holographically patterned structures. Figure 2a,b shows microscale arrays of star-shaped objects made by MPA-derived HL at different magnifications. The vivid diffraction color in the inset of Figure 2a verifies the presence of periodic structures on the wavelength scale. As shown in the SEM images (Figure 2c,d), microstructures with

[*] Dr. S.-K. Lee, H. S. Park, Prof. S.-M. Yang
National Creative Research Initiative Center for Integrated Optofluidic Systems and
Department of Chemical and Biomolecular Engineering, Korea Advanced Institute of Science and Technology
Daejeon, 305-701 (Republic of Korea)
E-mail: smyang@kaist.ac.kr
Homepage: http://msfl.kaist.ac.kr
Dr. G.-R. Yi
Korea Basic Science Institute
Daejeon, 305-333 (Republic of Korea)
Prof. J. H. Moon
Department of Chemical and Biomolecular Engineering, Sogang University
Seoul, 121-742 (Republic of Korea)

[**] This work was supported by a grant from the Creative Research Initiative Program of the Ministry of Education, Science and Technology for "Complementary Hybridization of Optical and Fluidic Devices for Integrated Optofluidic Systems." Partial support from the Brain Korea 21 Program is also appreciated. We thank T. H. Lee at KAIST for help with DNA experiments.

Supporting information for this article is available on the WWW under http://dx.doi.org/10.1002/anie.200901166.

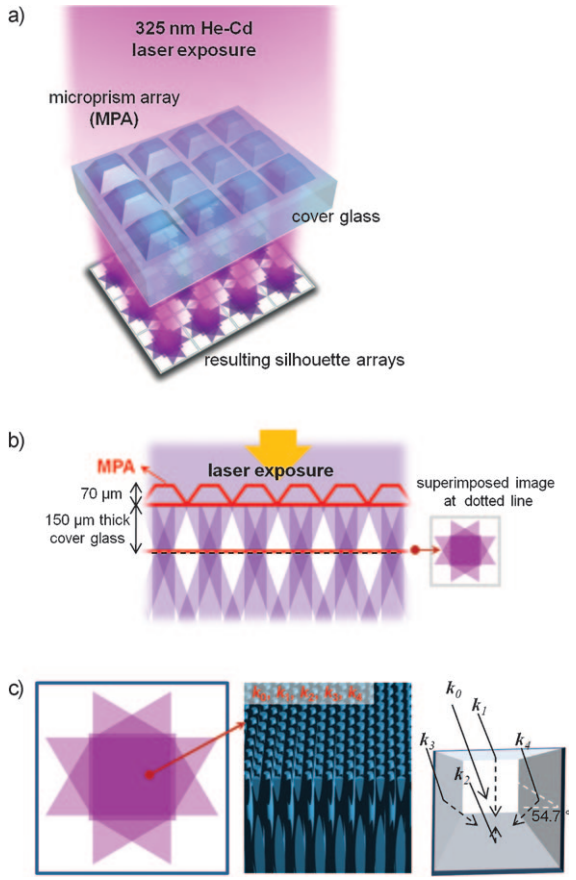

Figure 1. Schematic depiction of MPA-based HL. a) PDMS microprisms of square-pyramidal frustum shape were arrayed on a 150 μm thick microscope cover glass. In MPA-based HL, a single laser beam is split into an array of multibeams by an MPA with microscale features; the beams refracted by a single microprism create interference patterns with nanoscopic features. b) Refraction and overlapping of a vertically impinged laser beam through the MPA. Distinctly different overlapped silhouette images are created at different distances from the bottom of the MPA. The evolution of silhouette images is shown in Figures S2 and S3 in the Supporting Information. c) The interference silhouette at the bottom of the glass substrate has a star shape with extended edges, in which low-dimensional interference structures appear. However, 3D internal nanostructure is constructed by five-beam interference in the main central part. Each number in a subsection corresponds to the number of the overlapped beams. (For details, see Figure S2d in the Supporting Information). 3D five-beam interference nanostructures were illustrated by solving the interference equation with wave vectors $\boldsymbol{k}_0$–$\boldsymbol{k}_4$.

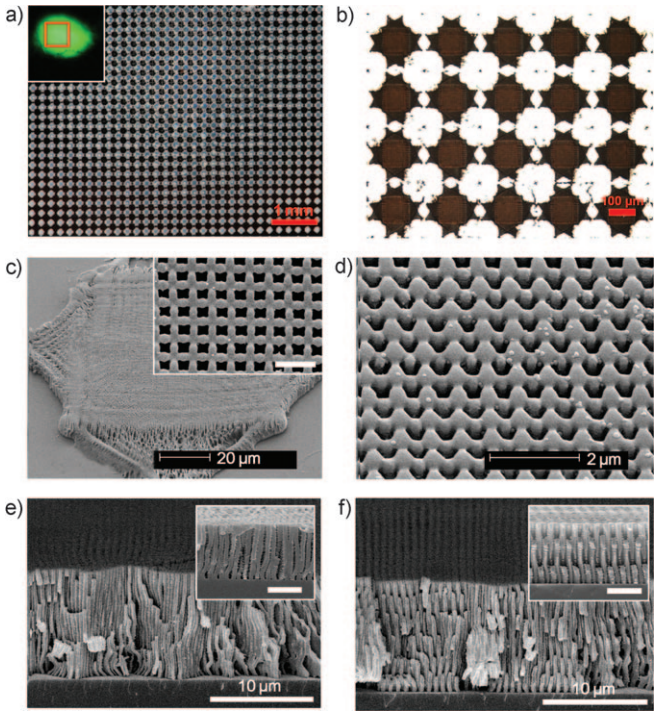

Figure 2. SEM and OM images of the resulting MPA-based HL structures. a) Large-area view of the microstructure array that occupies the red box in the inset. Inset shows vivid green diffraction from the periodic arrayed structure. b) Magnified OM image of 3D periodic microstructures with internal nanopatterns generated by truncated MPAs. c) SEM image of a single microstructure represented in (b). Inset: magnified top view. Scale bar is 1 μm. d) Tilted SEM image of the top surface of holographic structures in (b). e, f) Cross-sectional SEM images of MPA-derived 2D and 3D holographic structures, respectively. The 2D structure has a very high aspect ratio of 30:1. Images in the insets show the corresponding structures with a small aspect ratio of 13:1. Scale bars in the insets are 2 μm.

nanoscale square lattices were generated with 650 nm lattice constant and 350 nm pore size. Figure 2e,f shows cross-sectional SEM images of the 2D and 3D internal HL structures across the microstructures, respectively. As expected, the MPA-derived patterns exhibit internal structures with nanoscale periodicity. By adjusting the thickness of the photoresist film, the aspect ratio of the resulting structures could be modulated. Figure 2e shows the bundle of pillars with a high aspect ratio (30:1) that originated from three-beam interference. The interference of four or five beams created interconnected 3D structures with periodicity in the perpendicular direction (Figure 2f).

Owing to the structural effect, the MPA-derived microstructures displayed enhanced fluorescence when labeled with a fluorescent dye. Enhancement of fluorescence signal can be achieved not only by large surface area for binding of target molecules with fluorescent labels but also by well-organized pores for enhanced mass transport from the bulk phase to the binding sites. To this end, the microparticles should have large available surface area as well as interconnected macropores (with pore diameter of ca. 50 nm). Our MPA-derived microstructures with macropores satisfy these structural requirements for efficient fluorescent particles. For comparison, arrays of similarly sized squares were fabricated by photolithography to verify fluorescence enhancement. Both the MPA-derived microstructure arrays and conventional square arrays were fabricated under the same experimental conditions using the same batches, with rhodamine B as a label. Figure 3a,b shows comparative confocal microscopy images, for which all observation parameters were fixed at the same values. These show that the HL structures always exhibit clearer images than the photolithographic squares. Comparison of the intensity profiles (Figure 3c) indicates that the fluorescence of the MPA-derived structure was 14.3 times larger than that of a simple square. Based on the SEM image

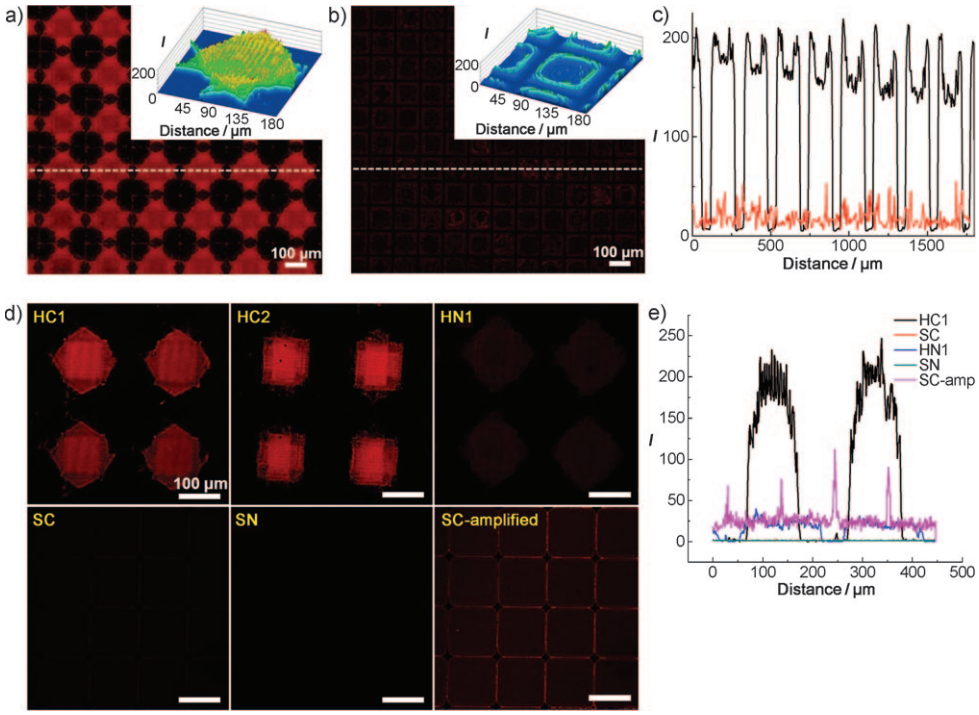

Figure 3. Confocal microscope analysis of arrayed structures treated with rhodamine B and Cy3-labeled DNA. a, b) Confocal microscope images of rhodamine B labeled holographic particle arrays (a) and photolithographic square particles (b) under the same observation conditions. Insets in (a) and (b) show the fluorescence intensity distribution of a single particle. The central parts of the star-shaped microstructures and the squares were 100×100 μm in size. c) The intensity profile of HL particle arrays (black) compared with photolithographic square particle arrays (red). Data were taken by scanning along the white dotted horizontal lines in (a) and (b). d) Confocal microscope images after hybridization of complementary or non-complementary probe DNA to the capture probe DNA located on the particle surfaces. Complementary and non-complementary probes were labeled with Cy3. HC1: positive control, HC2: positive control, HN1: negative control using HL-derived microstructure arrays of different shapes. SC: positive control, SN: negative control, SC-amplified: positive control with high gain using photolithographic simple squares. e) The intensity profiles obtained from the images HC1, SC, HN1, SN, and SC-amplified.

analysis, the surface area of the HL-driven macropore structure (9 m^2g^{-1}) was much greater than 0.14 m^2g^{-1} for the solid square array with no pores. The enhanced fluorescence was caused mainly by the structural advantages for chemical and biomolecular reactions. Furthermore, we conducted a complementary DNA-binding experiment to demonstrate the advantage of HL structures over the simple squares for detection of biomolecules. The set of pictures in Figure 3d shows the arrays of MPA-based HL structures and simple squares after hybridization of complementary or non-complementary probe DNA strands labeled with cyanine dye (Cy3). As noted, the high surface area and well-organized macropores of our MPA-based HL structures advantageously affected both capture probe binding and detective probe binding (Figure 3e); the fluorescent detection signal was enhanced dramatically and was 121.6 times stronger than that from simple squares. This result indicates clearly that our MPA-derived structures have strong potential for highly sensitive DNA or protein chips.[30,31]

The effectiveness of lithographic approaches has been demonstrated recently for the preparation of fluorescent particles with various shapes with no internal nanostructures.[27,28,32] However, fluorescent particles prepared by conventional synthesis or lithography techniques do not have the high fluorescence efficiency and other desirable properties displayed by natural diatomaceous particles, which have internal nanostructures.[5,9–13,33] We show how free-standing microparticles with internal nanopatterns could be released from the MPA-derived arrays by dissolution of a precoated sacrificial layer. A scheme for the fabrication of artificial diatoms is presented in Figure 4a. Figure 4b shows a large number of suspended particles with strong diffraction colors collected from only two laser spots. Dye-doped "artificial diatoms" with various external shapes were also produced for fluorescent particles (Figure 4c). It is noteworthy that mass production of microparticles with internal nanopatterns is possible using our HL-based approach. In 14 seconds of total laser exposure time, over 140000 particles could be created on a four-inch wafer (10^4 particles per second) in lab-scale systems. The polymeric "artificial diatoms" reported herein can not only replace conventional fluorescent particles in detection or diagnosis but could also be used as catalysts, microdiffraction gratings for sensors, and special pigments for cosmetics and paints.[9–13,33]

In summary, we fabricated arrays of microprisms from transparent PDMS elastomer and demonstrated that both multidimensional and multiscale structures could be prepared by MPA-based HL. In particular, a greater than 14 times increase of the fluorescence signal and 120 times enhancement of DNA detection efficiency were achieved from our MPA-based HL structures relative to those from simple solid systems. Using a sacrificial layer, artificial diatoms with advanced fluorescence properties were detached from the arrayed microstructures, potentially enabling application of artificial diatoms in a variety of biotechnology systems including bio-imaging and diagnostic detection and identification.

Experimental Section

Preparation of MPAs: Silicon masters for MPAs were made by anisotropic wet etching of (100) silicon wafers with an etching angle of 54.7°. (Gallery of MPAs and silicon master molds for MPAs are

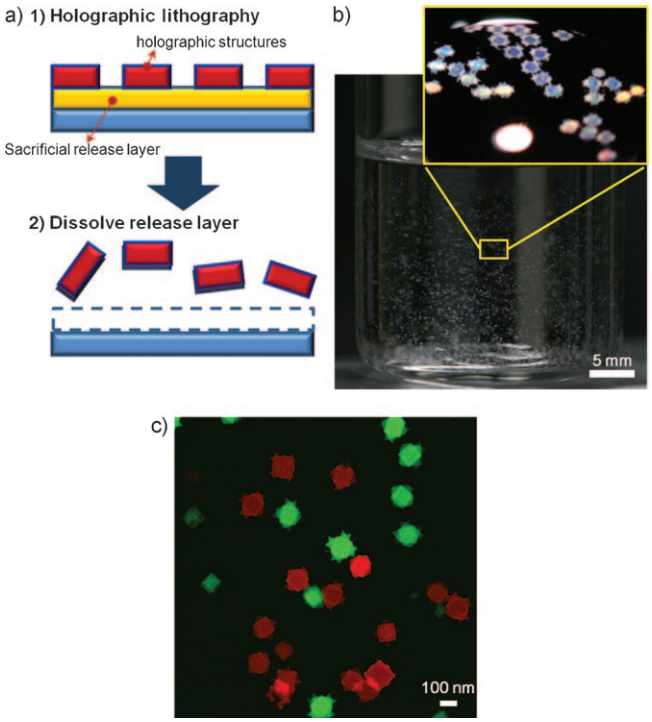

Figure 4. Fabrication of free-floating HL particles and multiscale silica particles with mesoporous structure. a) Scheme for the preparation of free artificial diatoms. b) OM image of nanostructured particles suspended in an aqueous solution contained in 10 mL glass vial. All particles were collected from only two laser spots. Inset: nanostructured particles in a single droplet exhibit various diffraction colors. c) Multichannel confocal microscope image of various nanostructured particles labeled with rhodamine B (red) and fluorescein isothiocyanate (FITC, green).

available in Figure S1 in the Supporting Information.) The shape of the pyramid top edge could be sharpened or truncated by controlling the silicon wet etching time. The dimensions of the truncated pyramid prism were determined by ray tracing (Figure S2a in the Supporting Information). Using the carved silicon substrates as master molds, MPAs made of transparent polydimethylsiloxane (PDMS 184-A and 184-B, Sylgard) were fabricated by soft lithography onto microscope coverslips (150 μm thick). Vaporized hexamethyl disiloxane (HMDS, Aldrich) was deposited on the silicon master substrate to form a self-assembled antiadhesion monolayer.

Holographic lithography: The optical setup for HL included a HeCd laser (CW, 325 nm, 50 mW, Kimmon) with a ×10 beam expander as a coherent light source. The final spot was around 1.2 cm in diameter. An electronic beam shutter was used to control the exposure time. A scheme for the optical setup is available in Figure S4a in the Supporting Information. To prepare a photoresist, an epoxy-based resin (SU-8, EPON) and a photoacid generator (PAG, triaryl sulfonium salts, Aldrich) were dissolved in γ-butyrolactone (GBL). After coating and soft-baking of the SU-8 resin, laser beams were passed through the MPAs. The laser exposure time ranged from 0.01 to 1.0 s, depending on the thickness and PAG content of the films. Finally, unexposed parts were removed by propylene glycol methyl ether acetate (PGMEA) and rinsed with isopropyl alcohol. Wave vectors of each beam are represented as $\boldsymbol{k}_i = 2\pi/\lambda\ (\cos\beta_i\sin\alpha, \sin\beta_i\sin\alpha, \cos\alpha)$. Here, λ is the wavelength of the laser and α and β_i are the polar and azimuthal angles of $\boldsymbol{k}_i$, respectively, as shown in Figure S4b. The set of electric field vectors $\boldsymbol{E}_0$–$\boldsymbol{E}_4$ used for the interference structure calculation is {−1(0, 0, 1), −0.99(0, 0.3310, 0.9436), −0.99(0, −0.3310, 0.9436), −0.83(0.3310, 0, 0.9436), −0.83(−0.3310, 0, 0.9436)}. Conformations of beams for other types of MPAs are also available in Figure S4 of the Supporting Information.

Fluorescence adsorption experiments and DNA-specific binding experiments: Rhodamine B, ZnS quantum dots, and FITC-labeled bovine serum albumin (BSA) were used as gain materials for observing fluorescence enhancement in microstructures with internal nanopatterns. The MPA-derived microstructures and photolithographic patterns were labeled with solutions of rhodamine B in ethanol (0.0467 wt%; HPLC grade, Merck), 0.22–0.33 wt% BSA in water, or 0.22 wt% quantum dots in hexane. For doping with the BSA solution, the MPA-based HL structures were treated with oxygen plasma to make the surface hydrophilic. After soaking in the solution for 30 min the samples were washed in ethanol for 24 h with gentle agitation, then rinsed several times with ethanol and distilled water. The results for ZnS quantum dots and FITC-labeled BSA are shown in Figure S5 of the Supporting Information. For the substrate for DNA immobilization, SU-8 structures were treated with 1M sulfuric acid solution to generate a large number of hydroxy groups on the surface. Then, hydroxy groups were substituted with amine groups using (3-aminopropyl)trimethoxysilane (APS, Aldrich). Single-strand DNA (10 μM) was spotted and incubated for 12 h for immobilization. Samples were exposed to UV light to confirm bonding of capture probe DNA (sequence for capture probe: 5′-CTA GGC GTT TGT ACT CCG TCA-3′). After washing twice, complementary or non-complementary DNA (100 nM) was dropped and incubated for 2 h for hybridization (sequence for complement probe: 5′-Cy3-TGA CGG AGT ACA AAC GCC-3′ and non-complementary probe: 5′ Cy3-ACA TCG GTC AAC GAA GAG-3′). Finally, samples were washed with buffer and ternary distilled water.

Preparation of free-floating particles: A sacrificial layer was placed between the photoresist and the substrate by spin coating at 6000 rpm. The sacrificial layer was removed in developer (MF 319, Microchem) for 1 min. Structured particles lacking sacrificial layers were all damaged during release (Figure S6 in the Supporting Information). For confocal microscopy observation, the artificial diatoms were labeled with rhodamine B and FITC before the development process.

Received: March 2, 2009
Revised: April 13, 2009
Published online: May 27, 2009

Keywords: fluorescence · laser chemistry · lithography · macroporous materials · microarrays

[1] A. R. Parker, H. E. Townley, *Nat. Nanotechnol.* **2007**, *2*, 347.
[2] P. Yang, T. Deng, D. Zhao, P. Feng, D. Pine, B. F. Chmelka, G. M. Whitesides, G. D. Stucky, *Science* **1998**, *282*, 2244.
[3] I. K. Sung, M. Mitchell, D. P. Kim, P. J. A. Kenis, *Adv. Funct. Mater.* **2005**, *15*, 1336.
[4] A. Khademhosseini, R. Langer, J. Borenstein, J. P. Vacantik, *Proc. Natl. Acad. Sci. USA* **2006**, *103*, 2480.
[5] J. H. Jang, D. Dendukuri, T. A. Hatton, E. L. Thomas, P. S. Doyle, *Angew. Chem.* **2007**, *119*, 9185; *Angew. Chem. Int. Ed.* **2007**, *46*, 9027.
[6] J. Henzie, M. H. Lee, T. W. Odom, *Nat. Nanotechnol.* **2007**, *2*, 549.
[7] C. Haynes, R. Van Duyne, *J. Phys. Chem. B* **2003**, *107*, 7426.
[8] M. Deubel, G. von Freymann, M. Wegener, S. Pereira, K. Busch, C. M. Soukoulis, *Nat. Mater.* **2004**, *3*, 444.
[9] A. Setaro, S. Lettieri, P. Maddalena, L. De Stefano, *Appl. Phys. Lett.* **2007**, *91*, 051921.
[10] H. E. Townley, K. L. Woon, F. P. Payne, H. White-Cooper, A. R. Parker, *Nanotechnology* **2007**, *18*, 295101.

[11] Z. Bao, M. R. Weatherspoon, S. Shian, Y. Cai, P. D. Graham, S. M. Allan, G. Ahmad, M. B. Dickerson, B. C. Church, Z. Kang, H. W. Abernathy III, C. J. Summers, M. Liu, K. H. Sandhage, *Nature* **2007**, *446*, 172.
[12] T. Lebeau, J. M. Robert, *Appl. Microbiol. Biotechnol.* **2003**, *60*, 624.
[13] B. Rapp, *Mater. Today* **2004**, *7*, 13.
[14] W. L. Barnes, A. Dereux, T. W. Ebbensen, *Nature* **2003**, *424*, 824.
[15] J. D. Joannopoulos, S. G. Johnson, J. N. Winn, R. D. Meade, *Photonic crystals: Molding the flow of light*. 2nd ed., Princeton University Press, Princeton, **2008**.
[16] S. Kim, J. M. Jung, D. G. Choi, H. T. Jung, S. M. Yang, *Langmuir* **2006**, *22*, 7109.
[17] D. G. Choi, H. K. Yu, S. G. Jang, S. M. Yang, *J. Am. Chem. Soc.* **2004**, *126*, 7019.
[18] A. G. Brolo, E. Arctander, R. Gordon, B. Leathem, K. L. Kavanagh, *Nano Lett.* **2004**, *4*, 2015.
[19] S. Jeon, E. Menard, J. U. Park, J. Maria, M. Meitl, J. Zaumseil, J. A. Rogers, *Adv. Mater.* **2004**, *16*, 1369.
[20] J. H. Moon, J. Ford, S. Yang, *Polym. Adv. Technol.* **2006**, *17*, 83.
[21] D. J. Shir, S. Jeon, H. Liao, M. Highland, D. G. Cahill, M. F. Su, I. F. El-Kady, C. G. Christodoulou, G. R. Bogart, A. V. Hamza, J. A. Rogers, *J. Phys. Chem. B* **2007**, *111*, 12945.
[22] D. Shir, H. Liao, S. Jeon, D. Xiao, H. T. Johnson, G. R. Bogart, K. H. A. Bogart, J. A. Rogers, *Nano Lett.* **2008**, *8*, 2236.
[23] Y. S. Nam, S. Jeon, D. J. Shir, A. Hamza, J. A. Rogers, *Appl. Opt.* **2007**, *46*, 6350.
[24] T. W. Lee, S. Jeon, J. Maria, J. Zaumseil, J. W. P. Hsu, J. A. Rogers, *Adv. Funct. Mater.* **2005**, *15*, 1435.
[25] S. Jeon, J. U. Park, R. Cirelli, S. Yang, C. E. Heitzman, P. V. Braun, P. J. A. Kenis, J. A. Rogers, *Proc. Natl. Acad. Sci. USA* **2004**, *101*, 12428.
[26] S. K. Lee, S. G. Park, J. H. Moon, S. M. Yang, *Lab Chip* **2008**, *8*, 388.
[27] S. Jeon, V. Malyarchuk, J. A. Rogers, G. P. Wiederrecht, *Opt. Express* **2006**, *14*, 2300.
[28] J. H. Moon, A. J. Kim, J. C. Crocker, S. Yang, *Adv. Mater.* **2007**, *19*, 2508.
[29] G. P. Wang, C. Tan, Y. Yi, H. Shan, *J. Mod. Opt.* **2003**, *50*, 2155.
[30] R. J. Lipshutz, S. P. A. Foder, T. R. Gingeras, D. J. Lockhart, *Nature* **1999**, *402*, 20.
[31] P. O. Brown, D. Botstein, *Nat. Genet.* **1999**, *21*, 33.
[32] C. J. Hernandez, T. G. Mason, *J. Phys. Chem. C* **2007**, *111*, 4477.
[33] J. H. Bang, S. H. Lim, E. Park, K. S. Suslick, *Langmuir* **2008**, *24*, 13168.

